Simulating polarisation diversity and power allocation in MIMO channels

L. Schumacher[1], J.P. Kermoal[1], K.I. Pedersen[2] and P.E. Mogensen[1, 2]

[1] Center for PersonKommunikation, Niels Jernes Vej 12, DK-9220 Aalborg East, Denmark
E-mail:{schum, jpk, pm}@cpk.auc.dk

[2] Nokia Networks, Niels Jernes Vej 10, DK-9220 Aalborg East, Denmark
E-mail:klaus.i.pedersen@nokia.com

Abstract

MIMO (Multiple Input Multiple Output) channels are known for some time now to offer either greater link gains or better spectral efficiency, depending on the correlation level of the scattering environment [1]. However, the benefits to be gained from the use of smarter antenna topologies do definitely not rule out gains available by the use of other techniques, such as polarisation diversity. The present paper investigates the benefits offered by this technique in an outdoor-to-indoor microcell scenario. More specifically, it corroborates previous conclusions drawn from measurements presented in [2] with the help of simulation results. These results have been produced using the COSSAP® implementation of a stochastic model of MIMO radio channels developed in the framework of European-funded IST (Information Society Technologies) METRA (Multi Element Transmit and Receive Antenna) project [3]. Moreover, two power allocation strategies are applied to the scenario under study and their performance is compared.

1 Introduction

Extensive work is currently ongoing to improve the capacity of wireless systems in order to accommodate the increasing customer demand for bandwidth-consuming value-added services. In this perspective, the use of multi-element transmit and receive antennas has been recently reported to be an efficient option in the open literature [1, 5, 6]. It is also discussed presently in standardisation forums like 3GPP (Third Generation Partnership Project) [4].

The MIMO (Multiple Input Multiple Output) radio channel resulting from this $N \times M$ concept, where N and M are the number of elements of the antenna array at the mobile station (MS) and at the base station (BS) respectively, can easily be represented as a transfer matrix $\mathbf{H}$. Its elements h_{nm} are the complex impulse responses of the channel connecting the n^{th} antenna at the MS to the m^{th} antenna at the BS.

The MIMO radio channel is known to provide $k \le \min(M, N)$ orthogonal subchannels[1], where the function $\min(.)$ returns the minimum value of the arguments. The capacity improvement that can be expected from the MIMO radio channel, i.e. the maximum number of k subchannels achievable, strongly depends on the spatial correlation properties between the elements of the antenna arrays. The more decorrelated they are, the more numerous the subchannels are, and the more spectrally efficient the whole system is. In turn, the correlation properties of the antenna elements strongly depend on the scattering properties of the transmission environment.

Preliminary experimental investigations in microcell environments [2] have empirically illustrated that polarisation diversity is an attractive solution to achieve decorrelated antenna elements. Systems implementing polarisation diversity do not only appear to be more efficient, they are also more robust, thanks to the fact that polarisation diversity relies on other physical properties than space diversity. Moreover, combining space and polarisation diversities produces more compact set-ups. This paper aims at corroborating these conclusions from [2] through Monte-Carlo simulations. On the other hand, the performance of two power allocation strategies applied to the system under study is compared.

2 Description

2.1 System set-up

It is believed that 2×4 set-ups are reasonable configurations of the $N \times M$ MIMO concept for mobile communications. Consider thus two such set-ups as shown in **Fig 1** and **Fig 2**. In both cases, the MS exhibits two antenna elements separated by half a wavelength. At the BS, two options have been

[1] Following the approach of [7], some authors upper bound k such that $k \le \min(M, N, Q)$ where Q is the number of simulated paths in a multipath environment. This limit does not apply here as real-life environments are considered.

considered, spatial separation only (**Fig 1**) and combined spatial separation and polarisation diversity (**Fig 2**). In the former case, antenna elements are regularly distributed so as to achieve half a wavelength separation between two adjacent ports. In the latter case, the BS is made of two pairs of two co-located elements separated by half a wavelength. The co-located elements use orthogonal polarisations (+45º, -45º).

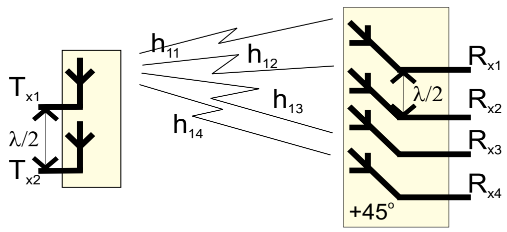

Fig 1 2×4 set-up with spatial diversity only

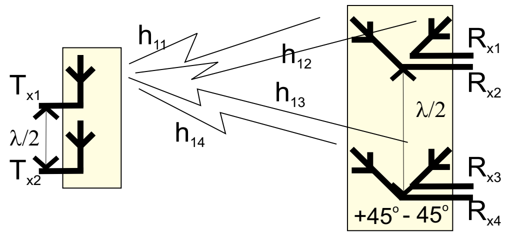

Fig 2 2×4 set-up with combined spatial and polarisation diversity

2.2 Simulations

The simulations have been performed using the COSSAP® implementation of a simple stochastic model of the MIMO radio channel described in [8]. The MIMO channel is modelled as a tapped delay line with taps computed such as to embed time dispersion, fast fading and spatial correlation. One of the most interesting features of this model is that it requires just a few parameters to completely characterise the scattering environment. Interestingly, sets of these parameters are either already available in the literature or easily extracted by post-processing of measurement results.

To simulate the set-ups under study, the stochastic model mentioned here above requires a description of the power-delay profile, of the time variation of the channel and of the spatial correlation between the elements at the MS and at the BS. Simulations have been performed considering a single tap channel model (narrowband signalling) with classical Doppler spread (Jakes). As far as the spatial correlation between elements is concerned, the values of the cross-correlation between elements at MS and BS were read from [9]. This reference gives values for the cross-correlation between antenna elements in a microcell environment, considering separately spatial separation and polarisation diversity.

With spatial separation only, the correlation matrices used as input of the COSSAP® model implementation were

$$\mathbf{R_{MS}} = \begin{bmatrix} 1 & 0.2 \\ 0.2 & 1 \end{bmatrix}$$

$$\mathbf{R_{BS,spatial}} = \begin{bmatrix} 1 & 0.96 & 0.87 & 0.74 \\ 0.96 & 1 & 0.96 & 0.87 \\ 0.87 & 0.96 & 1 & 0.96 \\ 0.74 & 0.87 & 0.96 & 1 \end{bmatrix}$$

for the MS and the BS respectively.

For the second case where both spatial separation and polarisation diversity[2] are applied at the BS, the resulting cross-correlation matrix $\mathbf{R}_{BS,spatial+polar}$ was computed as the product of the cross-correlation values related to each of the two options, spatial separation and polarisation diversity, considered separately, as suggested by [10]. This gave

$$\begin{aligned}\mathbf{R}_{BS,spatial+polar} &= \mathbf{R}_{BS,polar} \otimes \mathbf{R}_{BS,spatial} \\ &= \begin{bmatrix} 1 & 0.2 \\ 0.2 & 1 \end{bmatrix} \otimes \begin{bmatrix} 1 & 0.96 \\ 0.96 & 1 \end{bmatrix} \\ &= \begin{bmatrix} 1 & 0.96 & 0.2 & 0.192 \\ 0.96 & 1 & 0.192 & 0.2 \\ 0.2 & 0.192 & 1 & 0.96 \\ 0.192 & 0.2 & 0.96 & 1 \end{bmatrix}\end{aligned}$$

where $\otimes$ represents the Kronecker product.

As upper and lower limits to the performance of the set-ups under study, two other 2×4 set-ups have been simulated with the same tool. The first one was fully correlated

$$\mathbf{R}_{MS,correlated} = \mathbf{R}_{BS,correlated} = \mathbf{1}$$

while the other one was defined as fully uncorrelated

$$\mathbf{R}_{MS,uncorrelated} = \mathbf{R}_{BS,uncorrelated} = \mathbf{I}$$

where each element of $\mathbf{1}$ is equal to one whereas $\mathbf{I}$ is the Identity matrix.

[2] Branch power ratio is assumed to be equal to 0 dB.

3 Analysis of simulation results

3.1 Eigenanalysis

The outcome of the simulations was the file of the channel taps generated during each simulation. As a post-processing step, the eigenanalysis of the instantaneous correlation matrix $\mathbf{R} = \mathbf{H}\mathbf{H}^H$ of each 2×4 taps snapshot has been performed[3]. It enables to analyse the transfer matrix $\mathbf{H}$ and consequently, to identify the set of k orthogonal subchannels, whose power gains are the eigenvalues $\lambda_i, i = 1...k$ [1]. The cdf (cumulative distribution function) of the derived eigenvalues is presented in **Fig 3** for the four different set-ups under consideration. Also shown is a portion of the cdf of a Rayleigh distributed random variable (bold dashed curve).

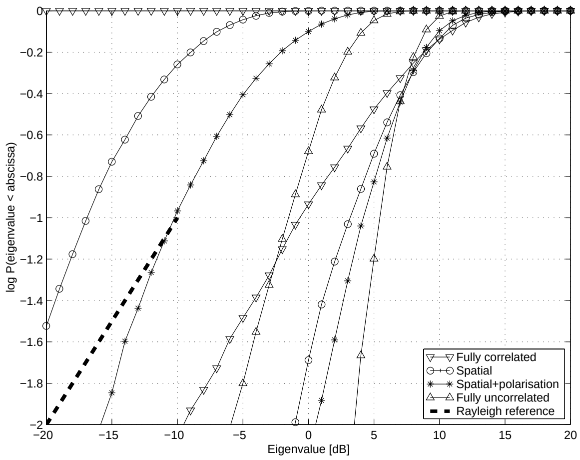

Fig 3 cdf's of the eigenvalues for the four considered set-ups

The fully correlated set-up only exhibits one significant eigenvalue, which illustrates that its channel matrix $\mathbf{H}$ is of rank one, or correspondingly, that only one subchannel is available. It is also worth noticing that the distribution of its eigenvalue is parallel to the Rayleigh reference. The expected link gain with respect to a 1×1 set-up amounts [11]

$$10\log_{10}(NM) = 10\log_{10}(2\times4) = 9\text{ dB}$$

which fully agrees with the simulation results. To the opposite, the fully uncorrelated set-up exhibits two significant eigenvalues, which account for two orthogonal subchannels. Both cdf's of these eigenvalues have greater slopes than the Rayleigh reference. This demonstrates that the subchannels corresponding to these eigenvalues are less impinged by fast fading than a typical mobile channel.

[3] $\mathbf{A}^H$ represents the Hermitian transpose of matrix $\mathbf{A}$.

The set-ups we are interested in, with mild correlation values, are in-between these two extreme cases. It can be noticed that both set-ups exhibit two significant eigenvalues. However, the set-up implementing both spatial and polarisation diversity has eigenvalues slightly stronger than the ones derived for the set-up relying on spatial diversity only. As stated in [2], a greater decorrelation is achieved between antenna elements at the BS thanks to polarisation diversity. This translates into more significant eigenvalues of $\mathbf{R}$.

3.2 Capacity estimation

The benefit of lower correlated set-ups becomes quantitatively explicit when turning these eigenvalues distribution into capacity curves. Indeed, the stronger an eigenvalue is, the more capacity the corresponding subchannel can deliver, as this eigenvalue can be regarded as the power gain of the corresponding subchannel. This is illustrated in **Fig 4**, which presents capacity[4] curves for the four considered set-ups.

These capacities have been computed from the eigenvalue distributions shown in **Fig 3** according to the relations given in [12]. Two different strategies have been applied as far as power allocation is concerned. The first, most obvious one is called "uniform". It allocates power on the transmitting antenna elements in a uniform, homogeneous way. This is a strategy to be applied when no knowledge about the channel can be used at the transmitter. However, when such knowledge can be inferred, smarter allocation strategies have been proposed, like the water-filling one described in [13]. Under some constraint

$$\sum_{i=1}^{k} P_i = P$$

it defines the power to be allocated to each of the k orthogonal subchannels identified from the eigenanalysis of $\mathbf{R}$ [1], as follows

$$\frac{1}{\lambda_1} + P_1 = \frac{1}{\lambda_2} + P_2 = ... = \frac{1}{\lambda_k} + P_k$$

Fig 4 depicts capacity computation results using both approaches at an operational SNR of 21 dB.

[4] The capacity expressions given throughout the paper are normalised with respect to the bandwidth, i.e. they are given in terms of bits/sec/Hz (spectral efficiency).

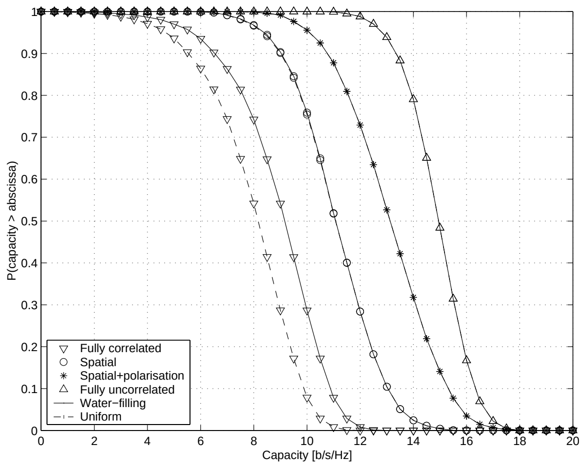

Fig 4 Complementary cdf's of the capacities for the four considered set-ups, with two different power allocation strategies

3.2.1 Polarisation diversity

Comparing set-ups, the extreme ones, fully correlated and fully uncorrelated, set the upper and lower limits of the considered system. At median, one measures a potential capacity increase of almost 8 bits/s/Hz. Thanks to decorrelation of the scattering environment, a 4 bits/s/Hz increase is already achieved in the case of the 2×4 set-up with spatial separation only. But an additional 2 bits/s/Hz is delivered by the combination of spatial diversity and polarisation, reaching a capacity of 13 bits/s/Hz at median.

3.2.2 Power allocation

Looking now at the power allocation strategies, the water-filling achieves 1 bit/s/Hz higher capacity than the uniform approach at median in the fully correlated case. For the sake of an intuitive explanation of this difference, assume that subchannels and antenna elements are matched. In this case, the uniform power allocation scheme wastes half the power as it allocates it to two sources whereas there is only one subchannel. On the contrary, the water-filling concentrates the available power on one single source. This generates a 3 dB improvement of the SNR in the case of the optimum, water-filling scheme, which translates into a 1 bit/s/Hz capacity difference.

However, the capacity difference between the power allocation strategies decreases as the environment becomes uncorrelated. The difference between the outcomes of the two different approaches is already hardly noticeable in the case of the set-up exhibiting only spatial diversity, as capacity curves start superposing. Obviously, as the second subchannel grows, the blind power allocation of the uniform scheme becomes less awkward. As illustrated qualitatively in **Fig 5**, the more correlated an environment is, the less spectrally efficient it is (low capacity), and the more different the outcomes of water-filling and uniform power allocation schemes are.

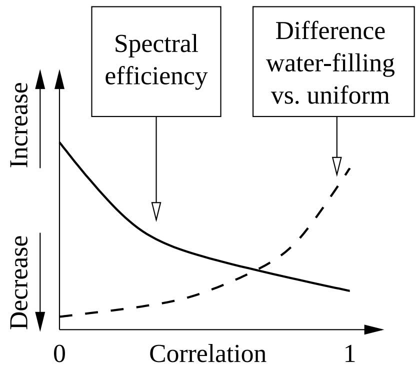

Fig 5 Qualitative comparison between spectral efficiency and power allocation schemes as a function of the correlation properties of the environment

4 Conclusions

Using simulation results, this paper has confirmed that polarisation diversity is a powerful and robust mean to build compact arrays whose antenna elements are decorrelated in a microcell MIMO scenario. Thanks to this technique, one can benefit from the capacity increase coming from the availability of orthogonal subchannels. It has also been shown that the water-filling scheme of power allocation outperformed the uniform one in correlated environments.

5 References

[1] J.B. Andersen, "Array Gain and Capacity for known Random Channels with Multiple Element Arrays at Both Ends", *IEEE Journal Selected Areas in Communications*, November 2000.

[2] J.P. Kermoal, P. Mogensen, S.H. Jensen, J. Bach Andersen, F. Frederiksen, T.B. Sørensen, K.I. Pedersen, "Experimental Investigation of Multipath Richness for Multi-Element Transmit and Receive Antenna Arrays", *IEEE Proc. 51th Vehicular Technology Conference*, pp. 2004-2008, Tokyo, Japan, May 2000.

[3] http://www.ist-metra.org

[4] Lucent Technologies, "Further Link Level Results for HSDPA Using Multiple Antennas", 3GPP TSG RAN WG1#17(00)1386, Stockholm, Sweden, November 2000.

[5] G.J. Foschini, "Layered Space-Time Architecture for Wireless Communication in Fading

Environment When Using Multi-Element Antennas", *Bell Labs Technical Journal*, pp. 41-59, Autumn 1996.

[6] I.E. Telatar, "Capacity of Multi-Antenna Gaussian Channels", AT&T Bell Labs, June 1995.

[7] G.G. Raleigh, J.M. Cioffi, "Spatio-Temporal Coding for Wireless Communication", *IEEE Transactions on Communications*, Vol. 46, No. 3, pp. 357-366, March 1998.

[8] K.I. Pedersen, J.B. Andersen, J.P. Kermoal, and P.E. Mogensen, "A Stochastic Multiple-Input-Multiple-Output Radio Channel Model for Evaluation of Space-Time Coding Algorithms", *Proceedings of VTC 2000 Fall*, pp. 893-897, Boston, United States, September 2000.

[9] European Commission ACTS Project Smart UNiversal BEAMforming (SUNBEAM), Deliverable 411 - 2-D Radio Channel Study AC347/AAU/A4/DR/P/001/11, pp. 54-93, July 1999.

[10] P.C.F. Eggers and J. Toftgaard and A.M. Oprea, "Antenna Systems for Base Station Diversity in Urban Small and Micro Cells", *IEEE Journal on Select Areas in Communications*, vol. 11, no. 7, pp. 1046-1057, September 1993.

[11] J.B. Andersen, "Antenna Arrays in Mobile Communications – Gain, Diversity and Channel Capacity", IEEE Antennas and Propagation Magazine, Vol. 42, no. 2, pp. 12-16, April 2000.

[12] European Commission IST Project Multi Element Transmit and Receive Antenna (METRA), Review and Selection of Relevant Algorithms, Deliverable D3.2 of IST-1999-11729 METRA Project, pp. 8-18, June 2000.

[13] R.G. Gallagher, "Information Theory and Reliable Communications", Wiley, 1968.